*Pure & Appl. Chem.*, Vol. 49, pp. 941 - 962. Pergamon Press, 1977. Printed in Great Britain.

# ADVANCES IN METHODS OF LIGHT-SCATTERING SPECTROSCOPY

B. Chu

Department of Chemistry, State University of New York
at Stony Brook, Stony Brook, New York 11794, USA

Abstract - We present here a survey on the progress of techniques and instruments of light-scattering spectroscopy in recent years. Emphasis is on advances made in photon correlation since 1974. A brief review on related fields, such as perturbed angular correlation measurements in nuclear physics, digital correlation in radio science, and laser Doppler velocimetry, is presented.

## I. INTRODUCTION

Light-scattering spectroscopy has made tremendous advances since the onset of laser. In a broader perspective, we can include Raman, Brillouin and Rayleigh scattering as well as newer developments of nonlinear optic effects. However, in its applications to macromolecules, only two branches of light-scattering spectroscopy, namely Raman and Rayleigh scattering, have become important tools. Yet, the field has grown so much that there is no consensus even among the experts concerning the scope of light-scattering spectroscopy. In this lecture, I shall limit my attention to areas which are related to mainly Rayleigh scattering and review the recent advances on high-resolution spectroscopic techniques, such as photon-correlation spectroscopy and Fabry-Perot interferometry. Furthermore, I shall emphasize on the practice of light-scattering spectroscopy.

The literature on Rayleigh-Brillouin scattering has grown to be enormous. There have been numerous reviews and monographs. Fleury and Boon (1) have listed over 500 references in their review article. Comparable number of references has appeared in my recent book on "Laser Light Scattering" (2). Aside from those references listed in (1) and (2), there have been at least six reviews (3-8), three books (2,9,10) and one conference proceedings (11) since 1974. The extent of such feverish activities also suggests that I should limit the present discussion to the more recent advances on light-scattering spectroscopy which are of interest to macromolecular science. Specifically, we shall be dealing with improvements on the methods of light scattering as well as advances made by scientists in other related disciplines, such as by engineers on laser Doppler velocimetry and by radio astronomers on digital correlation techniques. Due to an obvious lack of communication in such seemingly diversified fields, I have encountered on more than one occasion accomplishments claimed by one discipline while they have been published facts in another. Finally, it is my subjective viewpoint that the digital computer is a natural signal controller and processor for the type of information we seek in light-scattering spectroscopy. Consequently, there are many advantages in economy and versatility by utilizing one central processor which permits various types of light-scattering measurements.

In reviewing the advances on the methods of light-scattering spectroscopy, I have included
(II) light-scattering photometry because of its traditional importance in molecular weight, size and shape determinations of macromolecules in solution,
(III) Raman spectrometry for its more established role in polymer science and computer-controlled instrumentation,
(IV) Fabry-Perot interferometry because of its bridging effect in linking the frequency ranges of grating monochronometers and photon correlation,
(V) photon correlation which plays the major role on recent advances in macromolecular-motion studies by means of light-scattering spectroscopy, and finally
(VI) laser Doppler velocimetry which is closely related to electrophoretic light scattering.
Furthermore, the main discussions are on advances made since 1974 (2).

## II. ADVANCES IN LIGHT-SCATTERING PHOTOMETRY

Photon counting has become a fairly standard technique (2). Using ECL pulses and 100 MHz counters, it has a good dynamic range whereby no analog signals need to be considered. In light-scattering photometry, we deal with the more classical aspects of light scattering which includes measurements of angular distribution of scattered intensity and depolarization

ratios. It is a very powerful technique which can often give us information on molecular weight, size (radius of gyration), shape, intramolecular and intermolecular interactions of macromolecules in solution and represents the entire scope of what used to be known as light scattering. The method has sometimes been overlooked by those who practice the present-day light-scattering spectroscopy. It is possible to design an instrument which can measure the angular distribution of scattered intensity, depolarization ratios, and the spectral distribution of scattered intensity as a function of scattering angle without changing the mechanical elements of the setup. With an additional calibration standard, extrapolated zero-scattering angle zero-concentration integrated scattered intensity should yield information on the molecular weight.

Two aspects of recent developments in light-scattering photometry deserves our attention. One deals with scattering-intensity measurements at small scattering angles and the other concerns with the precision of angular intensity-ratio measurements.

II 1. Small-angle light scattering intensity measurements

Measurements of scattered intensity at small scattering angles ($\theta<30^{\circ}$) require us to consider carefully (a) the divergence of the incident beam, (b) the divergence of the scattered beam (c) surface reflection and refraction effects and (d) dust in the scattering medium. Condition (d) often becomes the limiting factor since it is most difficult to remove the dust particles from solutions. Small-angle light scattering of polymer solutions become essential whenever very large macromolecules, such as DNA, are being characterized. There, in order to obtain the proper extrapolated zero-angle scattered intensity and the limiting slope in a reciprocal scattered intensity versus $K^2$ plot, we need to make measurements down to $\theta\approx 5\text{-}10^{\circ}$. $K\{=(4\pi/\lambda)\sin(\theta/2)\}$ is the magnitude of the momentum transfer vector with $\lambda$ being the wavelength of light in the medium. Small-angle scattering intensity measurements together with simultaneous intensity values obtained at a large scattering angle (say, $\theta>80^{\circ}$) have been used in real-time particle sizing (13-14). The same optical geometry is applicable in electric-field light scattering of macromolecular solutions or colloidal suspensions when Doppler-shift measurements at small-scattering angles are desirable.

Fig. 1 shows a proposed schematic representation of one of the detection optics capable of small-angle light-scattering measurements. Using the thin lens optics, $1/(d_2+d_3) + 1/d_4 = 1/f$ where f is the focal length of lens L. the actual scattering cross-section at O is $\pi(d_1(d_2+d_3)/(2d_4))^2$ while the uncertainty of the scattering angle $\delta\theta_t = \delta\theta + d_1(d_2+d_3)/(d_2 d_4)+$ divergence of the incident beam. At small scattering angles, $\delta\theta_t/\theta$ often becomes a very important practical consideration and measurements at $\theta\sim 2^{\circ}$ are readily accessible. Linear translation of the annular scattering aperture permits measurements of scattered intensity at different scattering angles. The use of an annular aperture increases the efficiency of the collection optics. Aside from the movable annular scattering aperture which is not appropriate in flow velocity measurements, the optical geometry is identical to the symmetric heterodyne arrangement in laser Doppler velocimetry (15).

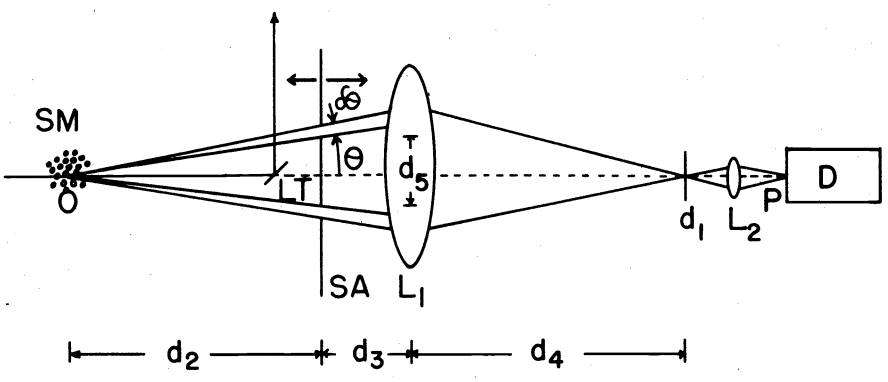


Fig. 1 A schematic representation of the detection optics capable of small-angle light scattering measurements. OP: optical axis; SM: scattering medium; OLT: incident beam; $\theta(=d_5/2d_2)$ scattering angle; $\delta\theta$: uncertainty in the scattering angle due to finite-size of the annular scattering aperture (SA); L: lens; $d_1$: pinhole which determines the scattering cross-section at O and adds to an uncertainty in $\delta\theta$; A: analyser; LT: light trap; D: detector. Linear translation of SA along the OP axis corresponds to a variation of the scattering angle.

II 2. Angular intensity ratio measurements

A precise determination of angular distribution of scattered intensity to about ± 0.1% using an incident wavelength of 488.0 nm at scattering angles approaching 15° and 170° represents a resolution of about 5 Å in the correlation length. Such an instrument should be useful in determining the radius of gyration of many biological macromolecules, such as proteins, and should compliment the small-angle X-ray scattering technique. For macromolecules with sizes in the range of say 50 Å, the solution-clarification procedure in fact becomes somewhat simpler as much more strigent measures, such as centrifugation of solution at very high speeds, can be utilized. Nevertheless, the dust problem remains a limiting factor in all such studies.

Lunacek and Cannell (16) developed an excellent analog ratio technique in their measurements of correlation length of carbon dioxide in the neighborhood of its critical point. A modified version using digital signal processing has been reported by S. P. Lee et al (17). Fig. 2 shows a schematic diagram of the digital photon-counting photometer. The three-channel scaler-timer is essentially a six-channel counter, each with a memory of 8 digits. Three channels are used for photon counting and the remaining three channels are used as corresponding timers derived from a 10 MHz crystal clock of stability ± 0.002%.

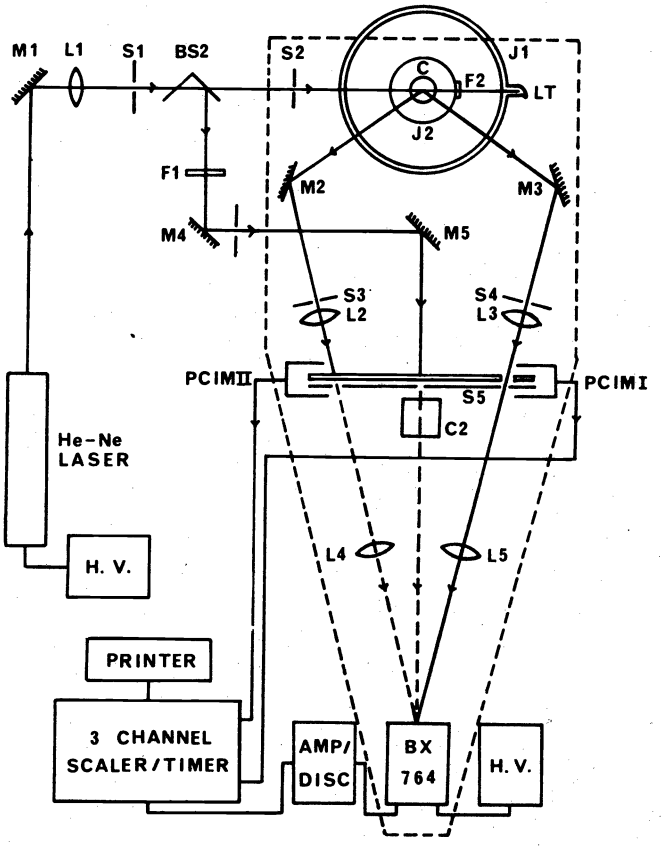


Fig. 2 A schematic diagram of the digital photon counting photometer (17). The notations are--M1-M5 are mirrors; L1-L5, lenses; F1 and F2, filters; S1-S5 diaphragms; BS2, a beam splitter; C2, a chopper; PCIM I and PCIM II, photon-coupled interrupter modules; J1 and J2, the outer and inner jacket of the thermostat, respectively. C is the sample cell, LT the light trap, HV the high voltage power supply, and EX764 the Bendix Channeltron tube. The dashed figure represents the aluminum plate on top of which is mounted the entire detector system.

The detection scheme was further improved and expanded to a six channel system using a multichannel scaler (18). Figure 3 shows a schematic representation of the photometer which measures the intensity of light scattered through four angles, of the reference and the transmitted beams. As the chopper wheel goes through one revolution the photo-multiplier (PM) tube sees each source for an equivalent time. The output from the PM tube is counted in a multichannel scaler (MCS) after proper pulse shaping. A photoelectric switch mounted on the chopper synchronously starts the MCS of each sweep.

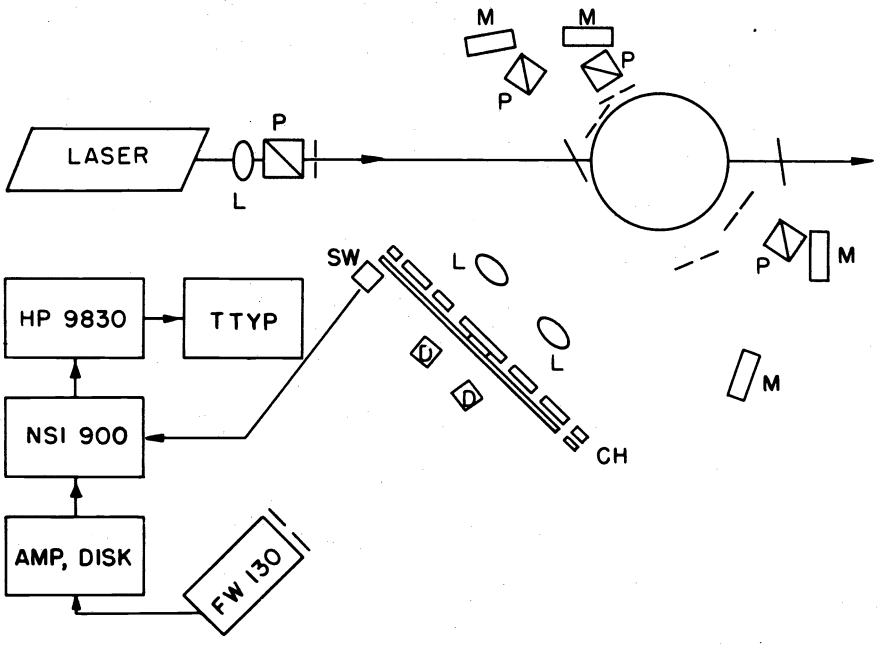


Fig. 3 A schematic diagram of the multiangle scattering photometer (18). Laser, Spectra Physics Model 124 He-Ne laser operating at 632.8 nm; L, lens; M, dielectric mirror; P, Glan-Thompson prism; CH, chopper; SW, switch; D, diaphragm; HP 9830, Hewlett-Packard Model 9830 calculator with 2K memory; TTYP, ASR33 teletype; NSI 900, Northern Scientific Model NS 900 multichannel analyzer; AMP, DISK, amplifier-discriminator; FW 130, ITT FW 130 photomultiplier tube. Typical pinhole size $\simeq$ 0.5 mm.

The total counts for each of the six "sources" are stored in different channels of the MCS memory as shown schematically in Fig. 4. After accumulating enough counts for each "source", the contents in the MCS memory are transferred to a Hewlett-Packard 9830 calculator for data analysis. We have set the chopper wheel such that the time for one revolution ($t_r$) is very slightly longer than the time for one sweep ($t_s$) by the MCS. The integrated intensity for each "source" is the sum of counts over a region of constant intensity as shown by a in Fig. 4. The drop in intensity as represented typically by region b of Fig. 4 is caused by partial closing of the detector aperture due to the chopper wheel in transit. The efficiency of the six-channel system can be represented by the actual measurement-time per sweep ($\equiv \sum_{i=1}^{6} a_i$) as compared with $t_r$. For the NS-900 MCS, there is an additional $\sim 4\mu$sec deadtime per channel. However, if we set the sweep time by say 5 msec per channel the total deadtime as well as the flyback time becomes unimportant (<1%).

In a very restricted way, the control mechanism of multi-angle photometers (17,18) has the appearance of resembling optical image processing by multiplex coding (19,20) even though, in fact, the control scheme presents a single detector being scanned sequentially. Fig. 5 shows a schematic representation of such a comparison. In terms of multiplex coding our choppers in Fig. 5 (a) and (b) are equivalent to an optical coder (Fig. 5 (c)) of very limited capability because it can only scan each channel (image point) sequentially one at a time. In the three channel system (17) as shown in Fig. 5 (a), we used a fairly complex control logic circuit together with outputs from photon-coupled interceptor modules as the electronic decoder while in Fig. 5 (b) the decoding was done by taking advantage of the sequential and synchronous nature of the MCS scan as well as the known MCS sweep time per channel. Fig. 5 (d) represents a proposed multi-angle multidetector photometric system where the optical coder can be shutters controlled by a digital computer via relay switches

and the code generator as well as the decoder can be provided by more flexible softwares. For example, the sample times for different "sources" including different scattering angles, the reference beam, the transmitted beam, the dark counts, etc. can be adjusted to provide the desired counting statistics.

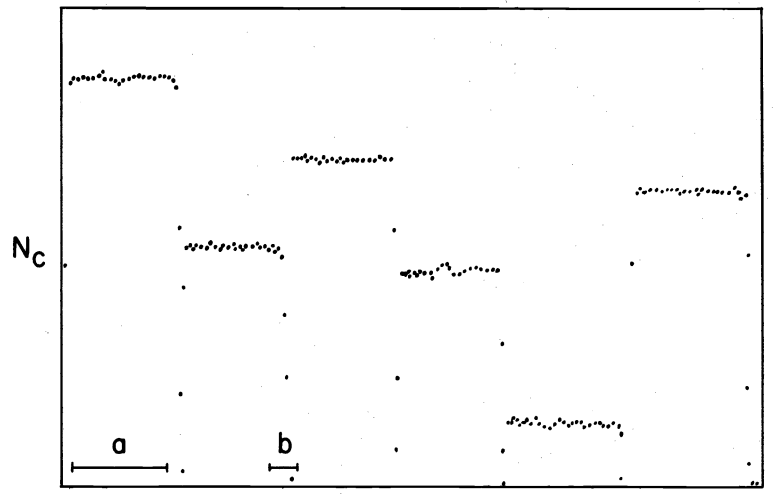


Fig. 4 A typical display from a multichannel scaler using the photometer of Fig. 3. $N_c$ is the total number of counts per channel; $a_i$ represents a region of constant intensity and shows the duration when a chopper hole is fully open; $b_i$ represents the deadtime when the optical geometry of the system is not precisely defined, i.e., the chopper hole is either fully or partially closed. The efficiency increases as $\sum_i b_i$ decreases.

Optical multiplexing (19,20) seems to have been first proposed by Golay (21) and is a means of making simultaneous measurements of different spectral elements in the output of a spectrometer using only a single detector. In Fig. 5 (c), separate orthogonally coded elements of an image (in our case, each element could correspond to viewing the scattering volume at a particular scattering angle) are first combined and detected in a single photodetector and then reconstructed back into the separate elements by cross correlation of the signal with the original codes. Multiplex advantage becomes obvious as the required number of elements (scattering angles) for the experiment increases. The sample time should be long when compared with the characteristic intensity fluctuation time ($1/\Gamma$) so that intensity fluctuations for each element give a Poisson distribution of photoelectrons (22).

The advantages and limitations of optical image processing by multiplex coding for photon-counting operation in both the signal- and dark-count domains have been discussed in detail (19). It is a recent development in terms of photon-counting operation so that I am not aware of any applications to light-scattering photometry or Fabry-Perot interferometry.

## III. ADVANCES IN RAMAN SPECTROMETRY

Using high-powered-laser sources and photon counting, commercial Raman systems, such as the Spex computer-driven Ramacomp (23,24), have sufficiently advanced designs that they approach state-of-the-art sophistication in Raman spectrometry. Recent advances offer mainly slight refinements in the detection system (25), such as compensation for both source and sample fluctuations (25,26) and provision of an internal reference standard which permits determination of a multiplicative instrument constant without an absolute intensity measurement. All the refinements can easily be adapted by the Spex system. However, hardware automated systems (25,26) are likely to be less flexible than computer-controlled software automated systems (24,27). Fig. 6 shows a typical system organization. The central processor unit (CPU) can be either a minicomputer, such as DEC PDP-11, (23,27) or even a calculator, such as HP-9830, (23) which has a built-in magnetic tape cassette. The Hewlett-Packard calculators (9825 or 9830) are quite adequate for equipment control, data aquisition and most of data analysis whenever the rate of transfer between the detector and the calculator can be acceptably slow. They are easy to use and offer ready-made interfaces for HP counters, DAC, multimeters, printers, plotters, etc. By linking the stepping motor drive with the double-grating monochrometer and controlling the counter gate, the CPU can automatically record intensity in number of photoelectron pulses per gate time versus frequency in wavelength or wave number. The same system can be used for automatic digital data

acquisition of angular distribution of scattered intensity as we have discussed in light-scattering photometry (II). The only difference is that we now connect the stepping motor drive to a turn-table or a translation stage instead of a double-grating monochrometer. The key-word is computer-control since I shall refer to the identical system organization in Fabry-Perot interferometry (IV) and light-beating spectroscopy (V). Therefore, in many light scattering laboratories, it should be more economical to use the computer-controlled approach rather than hardware systems. Aside from biological (28,29) applications, computer-controlled Raman spectrometers are capable of measuring weak spectra from opaque surfaces (30) and for determining stable isotope abundances (31). The calibration of a scanning monochromator can be achieved using "channel spectra" from a Fabry-Perot etalon to better than 0.05 $cm^{-1}$ at any point in the scan (32).

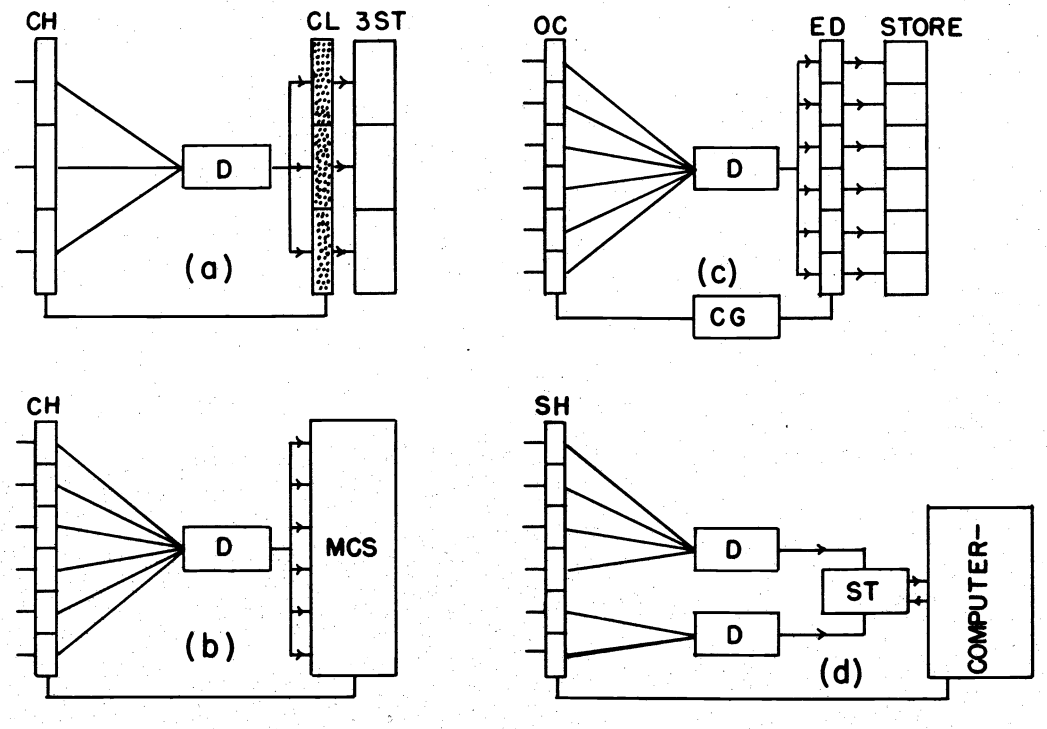


Fig. 5 A schematic representation of multiangle photometric detection systems as compared with an optical-multiplex system.

a) 3-channel photometer of Fig. 2. CH, chopper; CL, control logic circuit; 3S-T, 3-channel scaler/timer; D, detector.
b) 6-channel photometer of Fig. 3. MCS: multichannel scaler.
c) an optical-multiplex system using a single code generator. OC: optical coder, CG: orthogonal code generator; ED: electronic decoder; S: scaler.
d) a proposed multiangle-multidetector system which is computer-controlled. SH: shutter controlled by computer software; ST: scaler-timer controlled by computer software which can also act as a decoder and store.

## IV. ADVANCES IN FABRY-PEROT INTERFEROMETRY

The Fabry-Perot (F-P) interferometer has an extremely high resolving power when it is compared with the standard optical dispersing element, i.e., the grating monochromator. It has been used for precise wave-length measurements (32) as well as for Brillouin, and Rayleigh scattering of gases, liquids, solutions, and solids (2,33). For macromolecular solutions, the Fabry-Perot interferometer has seen only limited usage (34). Nevertheless, it is an important piece of equipment because its resolving power bridges that of a grating monochrometer and the electronic beating technique of optical mixing spectroscopy.

Construction of the F-P interferometer has now been well-developed that relatively stable

F-P interferometers which are quite adequate for use in laser light scattering are available commercially (35). In fact, in a polymer-science laboratory it will be quite difficult to construct a laboratory-built F-P interferometer which can exceed the thermal and mechanical stabilities of some of the better-made commercial ones. Since the main application of the F-P interferometer deals with depolarized Rayleigh scattering which yields information on the rotational motion of small macromolecules in solution, further advances which are of interest to us have been on changing the open-loop F-P interferometer into a closed-loop stabilization system. Although the pressure-scan method represents a time-tested approach to scanning the wavelength by changing the index of refraction between the interferometer plates, the advances in providing some averaging technique for piezoelectric-scanned F-P interferometers have been of main concern. Two schemes have been made available--one deals with servomechanisms for maintaining the F-P cavity alignment and axial cavity separation, the other utilizes a zero-crossing discriminator.

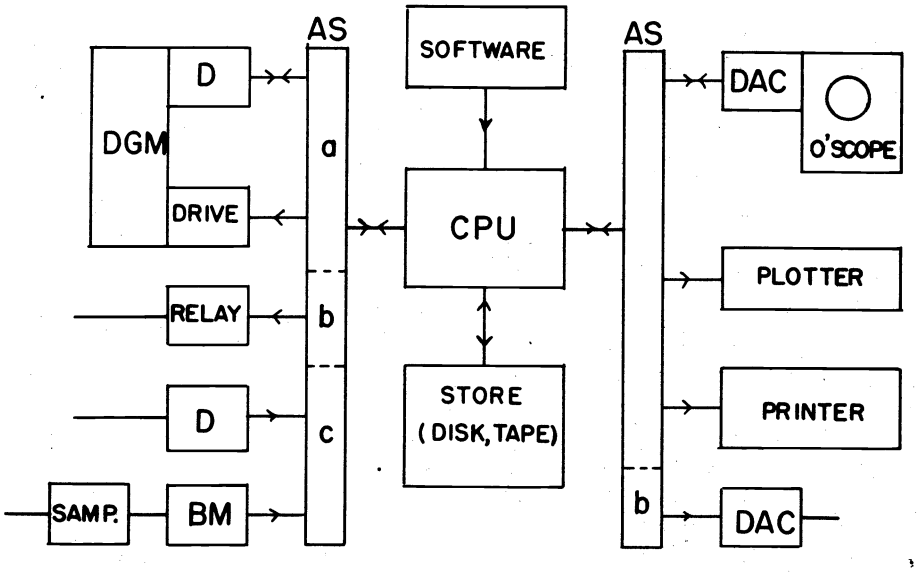


Fig. 6 A typical system organization. D consists of PM tube, preamplifier-amplifier/discriminator, and counter-timer; AS: address selector; BM: fast buffer memory; DAC: digital-to-analog converter; DACs are required for all analog output devices. CPU: PDP-11, or HP 9830. Software includes automatic control of experiment, data acquisition and analysis. Section AS(a) for a Raman spectrometer; AS (a) and (b) without DGM for a F-P interferometer servo; AS (c) for a software correlator.

IV 1. Servo mechanisms of F-P interferometer

Several successful servo schemes have been reported (36-39). The McLaren-Stegeman (38) scheme has been developed commercially by Burleigh Instruments, Inc. (23) as DAS-1 F-P data acquisition and stabilization system and DAS-10 F-P stabilization system. The scheme will be described briefly here since it represents a typically successful servo scheme. The servo mechanism uses the spectrum itself to indicate the error corrections and operates with a 3-element piezoelectric scanned F-P interferometer. It differs from the zero crossing averaging scheme which requires a reference laser beam. Fig. 7 shows a schematic diagram of a Brillouin spectrum of a liquid (40). After the interferometer has been aligned manually, the counts during one sweep of the ramp from data windows (1+2) and (3+4) are compared. A feed-back circuit on the voltage-bias of all three piezoelectric-transducer (PZT) elements will try to equalize the number of counts in (1+2) and (3+4). The net effect corresponds to stabilizing the F-P cavity separation and laser frequency drift. In alignment corrections, the feed-back circuit operates on two separate individual PZT elements, one at a time. The total number of counts during one sweep of the ramp from windows (2+3) are accumulated in a register. During the flyback following the ramp, a small voltage step is applied to one of the two PZT elements, causing the F-P alignment to change very slightly. During the next sweep, the total counts from windows (2+3) are accumulated in a second register. During the flyback following the second sweep of the ramp the counts in the two registers are compared and a small correction voltage whose polarity tends to maximize the number of counts is applied to the F-P interferometer. During the next two sweeps the process is repeated but applied to the second PZT element. Thus, the system continually checks and optimizes the F-P alignment. In principle, the system organization illustrated in Fig. 6 permits software control of all functions we have stated for DAS-1 and all of its options such as mode-hop control, segemented ramp, data smoothing, etc. The DAC outputs (Fig. 6) can be converted to a ramp voltage as well as voltage bias for the PZT elements by means of high voltage operational amplifiers.

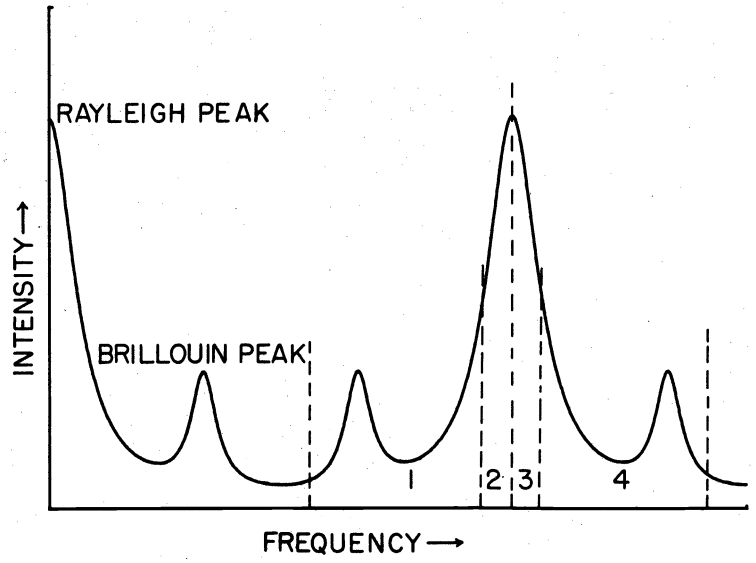


Fig. 7 A schematic representation of Brillouin scattering of a simple liquid. By equalizing the counts in data windows (1+2) and (3+4), the Fabry-Perot cavity separation and laser frequency drift are stabilized. By maximizing the total number of counts in windows (2+3), the cavity remains aligned for finesse optimization.

IV 2. Zero-crossing signal-averaging scheme

In a zero-crossing signal-averaging scheme, we have made no attempt to stabilize the F-P interferometer (41). Rather, we have taken advantage of the stability of present-day F-P interferometers and scanned the spectrum using a data collection period which is short when compared with the short-term laser and F-P frequency drifts. The zero-crossing scheme utilizes a reference laser beam which is independent of the scattered light. Thus, it works very well for weak spectra where signal-averaging becomes essential. Fig. 8 shows a typical block diagram of how a zero-crossing discriminator is incorporated into a signal-averaging scheme for Rayleigh-Brillouin scattering. The F-P interferometer is first scanned quickly across the laser reference frequency. The zero-crossing discriminator differentiates the output signal. At the maximum of the reference peak, it triggers the MCS and activates the chopper (CH) to block off the reference beam so that only the scattered beam is detected and recorded by the MCS. For the remaining portion of the sweep the ramp generator (RG) drives the F-P interferometer at a much slower rate and synchronously provided sample pulses to advance the MCS channel addresses. The fast/slow sweep rate corresponds to the segmented ramp option of DAS-1. The detailed hard-wired circuits have been reported elsewhere (41). Again if we examine the system organization of Fig. 6 closely, we see that all the functions for the zero-crossing signal-averaging scheme can be performed by the computer software control. The software control can have further options of combining schemes (1) and (2) or utilizing other types of minor variations (34) depending upon the nature of the experiment. Thus, the versatility of utilizing the type of system organization such as Fig. 6, can easily be appreciated. New designs and performance of high-stability F-P interferometers (42,43) and etalons (44) as well as a method for finding the instrumental profile of a F-P etalon (45) have been reported. However, these specific improvements are of little interest in the present context since commercial instrumentation on F-P interferometry is sufficiently adequate for Rayleigh-Brillouin scattering of macromolecules in solution and in bulk.

## V. ADVANCES IN PHOTON-CORRELATION SPECTROSCOPY

The practice of photon correlation has been discussed at both elementary (2) and more advanced (11) levels. Photon-correlation processes the signal in the time domain while spectral analysis operates in the frequency domain. Jakemann (11) has properly classified the techniques according to whether they are single or parallel channel methods. Table 1 lists the classification of instruments available for time-correlation or frequency-spectrum measurements. The wave (or spectrum) analyzer filters out one frequency component from a particular sample of signals at a time. For ten frequency components, it needs ten samples of signals. Similarly, the delay coincidence multiplies the intensity at one time by that at a preset delay time. For ten delay times, it needs ten such operations. The single start-single stop techniques make inefficient use of the signal since only one frequency or one time-delay component is measured from each sample of signals. Thus, the parallel method which measures x frequency or x time-delay components from each sample of signals

increases the efficiency of measurement time by a factor of x and improves the signal-to-noise ratio. A compromise for the single-channel instrument would be to record (51) the sample of signals and analyze the same sample at each frequency or time-delay component. Such a procedure can reduce the experiment time comparable to the parallel method but increases the analysis time by a factor of at least x. The computer approach in light-scattering spectroscopy essentially utilizes this advantage. All commercially available hardware wave- and spectrum-analyzers accept mainly analog signals. The inherent digital nature of photoelectron pulses should give an edge to those instruments which accept a digital input and carry out the analysis digitally. Consequently, we shall be concerned mainly with photon correlation.

In this section, I shall concentrate on two aspects of photon correlation. One measures the arrival times of photoelectron pulses; the other concerns with measurements of number of photoelectron pulses per sample time which is short when compared with the characteristic time of the signal of interest. Most commercial correlators have capabilities to make probability density function or photoelectric counting distribution (52) measurements. The construction of a simple analog device for such measurements has also been reported (53). However, our main interest in studying dynamical properties of macromolecules in solution is based on a more direct measure of the time-correlation function.

V 1. Arrival times of photoelectron pulses

There have been no recent advances in hardware instrumentation on determining intensity correlation functions using arrival times of photoelectric pulses. The technique seems to have originated in nuclear physics and has been popular in perturbed angular correlation (PAC) measurements which, for example, can be related to magnetic moments of short-lived excited nuclear states (54-56). It is capable of measurements at very short delay times, e.g., 1 nsec per channel which is about 50 times shorter than the fastest commercial Malvern correlator (23), is continuously being refined (57) and routinely used (58) by nuclear physicists. An interesting observation is that neither discipline, i.e., the laser physicists and the nuclear physicists, seems to be very much aware of the advances made by the other discipline since there are few cross references. For example, a long-period time-to-pulse height converter (59) was developed for half-lives in the range of μsec to sec while it could be quite possibly better to use a digital correlator which has already been developed at the time.

The use of a time-to-amplitude converter (TAC) together with a pulse-height analyzer (PHA) for photon time-of-arrival measurements has been explored (60-62). The method has several advantages because the TAC processes individual photoelectron pulses and therefore is able to make correlation measurements on very weak optical fields. Secondly, as we have already stated, it is capable of making photon correlation measurements of very short delay times. In this respect, the range is appropriate for making measurements on the rotational motion of small macromolecules in solution. Unfortunately, all previous reviews and books (1-11) have neglected this method with few listed references (2).

Davidson and Mandel (61) has presented a detailed mathematical analysis of the operation of the TAC. Davidson (62) developed a procedure for the measurement of second-order $\langle I(\underline{x},t)I(\underline{x},t+\tau)\rangle$ and third order $\langle I(\underline{x},t)I(\underline{x},t+\tau_1)I(\underline{x},t+\tau_2)\rangle$ intensity correlation functions with the use of a TAC. The essential features are summarized as follows.

In a stationary optical field, the two-fold joint probability function $p(x_1,t;x_2,t+\tau)$ that a photoelectron pulse from a photodetector located at $x_1$ appears in the 'start' channel at a time within t and t+ $\delta t$ and another photoelectron pulse from a second photodetector located at $x_2$ appears in the 'stop' channel at a time within $t+\tau + \delta\tau$ depends only on $\tau$ and is given by (63,64)

$$p(x_1,t;\, x_2,t+\tau) = \alpha_1\alpha_2 C^2 S_1 S_2 \delta t \delta\tau \langle I(x_1,t)\, I(x_2,t+\tau)\rangle \qquad (1)$$

where $I(x_1,t)$ and $I(x_2,t)$ are the light intensities located at $x_1$ and $x_2$ from photodetectors expressed in units of photons per unit volume, $S_1$ and $S_2$ are the surface areas and $\alpha_1$ and $\alpha_2$ are the dimensionless quantum efficiencies of the two photodetectors. C is a proportionality constant, the bracket $\langle\rangle$ represents a time (or ensemble) average and the expression $\langle I(x_1,t)I(x_2,t+\tau)\rangle$ is a cross-correlation function. In order for the TAC to register a time interval $\tau$, it is necessary not only that a 'stop' pulse appears $\tau$ seconds following the 'start' pulse, but also that no other 'stop' pulses occur within $\tau$. The modified two-fold joint probability function $\tilde{p}(x_1,t;x_2,t+\tau$: all other intervals) for a start pulse at $x_1$ and t, a stop pulse at $x_2$ and $t+\tau$, and no stop pulses at intervals $t_i$ with i=1,2,....,$N_o$ $(=\tau/\Delta\tau)$, is given by

$$\tilde{p}(x_1,t;x_2,t+\tau\text{: all other intervals}) = \alpha_1\alpha_2 c^2 S_1 S_2 \delta t \delta\tau \langle I(x_1,t)I(x_2,t+\tau) \prod_{j=1}^{N_o} [1-\alpha_2 c S_2 \Delta\tau I(x_2,t_j)+O(\Delta\tau)^2]\rangle \tag{2}$$

Thus, in the limit $N_o \to \infty$, we have for the counting probability of the TAC,

$$\lim_{N_o\to\infty} \tilde{p}(x_1,t;x_2,t+\tau\text{: all other intervals}) = \alpha_1\alpha_2 c^2 S_1 S_2 \delta t \delta\tau \langle I(x_1,t)\, I(x_2,t+\tau)\exp[-\alpha_2 c S_2 \int_t^{t+\tau} I(x_2,t')dt']\rangle \tag{3}$$

The difference between Eqs. (1) and (3) become important when the mean number of counts, $\langle \alpha_2 c S_2 \int_t^{t+\tau} I(x_2,t')dt'\rangle$ registered in the time interval is of order or greater than unity. By taking into account a number of deadtime effects, Davidson and Mandel (61) devised a quantitative expression for the modified two-fold joint probability

$$R(\tau=i\Delta\tau) = \Delta\tau\langle n(x_1,t,\Delta\tau)n(x_2,t+i\Delta\tau,\Delta\tau)\exp[-\int_{t-T_L}^{t+i\Delta\tau} n(x_2,t')dt'] \tag{4}$$
$$*\exp[-\int_{t-T_w}^{t} n(x_1,t')dt']\rangle\exp[-(\text{TAC conversion rate})\,(\text{deadtime})]$$

where $n(x_1,t,\Delta\tau)$ is the number of photoelectron pulses at position $x_1$ and time t per sample time $\Delta\tau$, $T_L$ is the delay introduced in the TAC stop channel so that registration of simultaneous arrival of start and stop pulses in channel 0 of the pulse-height analyzer will not occur, $T_w$ is the conversion range in seconds of the TAC. The effective deadtime of the TAC is not constant but is a function of delay time $\tau$ and can be very roughly expressed as $T_D+\langle\tau\rangle-T_w$ with $\langle\tau\rangle$ being the mean delay registered. For uncorrelated intensity fluctuations, $R(\tau)$ reduces to $R_u(\tau)$:

$$R_u(\tau) = \Delta\tau\langle n(x_1)n(x_2)\rangle\exp[-\langle n(x_2)\rangle(T_L+\tau)-\langle n(x_1)\rangle T_w] \tag{5}$$
$$*\exp[-(\text{TAC conversion rate})(\text{deadtime})]$$

The second-order intensity fluctuation correlation function for two photodetectors viewing the same point of the optical field, as shown schematically in Fig. 9, can be represented by an integral equation, with the zeroth-order solution taken to be $\xi(\tau)$.

$$\xi(\tau) = (R(\tau) - R_u(\tau))/R_u(\tau) \tag{6}$$

for $\tau_{max}\langle n(x)\rangle$ very small when compared with unity. $\tau_{max}$ is the maximum measurement time interval. The detailed procedure has been described by Davidson (62).

Formulation of time interval statistics in terms of the single-fold generating function with negligible dead times has been considered by Glauber (65) and Blake (66). In the case of a single exponential decay, Blake (66) obtained an analytical form for the probability density function. Thus, the characteristic correlation time can be determined more easily than by means of an integral equation.

The appearance of exponential factors in Eq. (5) is an obvious disadvantage of the method. Chopra and Mandel (67) have developed a correlator based on digital storage of the arrival times of up to six photoelectron pulses following a start pulse. The distribution of arrival times is a direct measure of the distribution of time intervals, which is proportional to the correlation function $\langle n(t)n(t+\tau)\rangle$. In practice, the probability $p(>N)$

that more than N counts are received in the given measurement interval $\tau_{max}$ must be kept very small. In the absence of intensity correlations,

$$p(>N) = \frac{(<n(t)>\tau_{max})^N}{N!} e^{-<n(t)>\tau_{max}} \left(1 + \frac{<n(t)>\tau_{max}}{N+1} + \frac{(<n(t)>\tau_{max})^2}{(N+1)(N+2)} + \dots\right) \quad (7)$$

Then, $p(>6)<10^{-3}$ for $<n(t)>\tau_{max}\approx 1$. In a $N_o$-channel pulse-height analyzer, $\tau_{max}=N_o\Delta\tau$. For a 4-channel time-to-digital converter (68), we get $p(>4)<2\times10^{-3}$ when $<n(t)>\tau_{max}\sim 0.5$. Thus when compared with the TAC technique we can tolerate appreciably higher counting rates with even only 4 consequetive arrival times.

V 2. Digital correlators

In surveying the advances in photon-correlation spectroscopy, I have come across interesting contributions made by radio astronomers who have been using the one-bit correlation technique to measure the spectra of radio astronomy signals for more than ten years (69-71). Although their emphasis is quite different from studying macromolecular dynamics, it is worthwhile to briefly review their work as their contributions have been neglected virtually completely by previous reviews and monographs. In this section, I shall (a) briefly summarize the contributions made by radio astronomers, and discuss recent advances in (b) hardware correlators and (c) computer-controlled systems.

V 2(a). Brief survey of digital-correlation techniques in radio-astronomy. The one-bit or polarity coincidence correlation method has become a widely accepted technique in radio astrophysical spectral line measurements. It was first used by Goldstein (71) in 1961 to study characteristics of radar echoes from Venus. Aspects of digital correlation techniques as applied to radio astronomical signals have been discussed by a number of authors (70-76). Although the one-bit correlation method (70,72,77-79) entails a theoretical loss of sensitivity, its simplicity and stability have made the technique more popular than multibit systems (73). Lately, however, more sophisticated designs such as a 1024-channel digital correlator (80) and multipulse correlators (81-83), have been reported. Hagen and Farley (84) have presented an excellent review on "Digital-correlation techniques in radio science."

In real-time signal processing the rates at which the products must be formed and stored for the correlation function estimate are far beyond the speed of present-day general purpose computers. Two general techniques, used either separately or together, have been applied to overcome this difficulty. One is to use hardware special purpose correlators and the other is to use coarse quantization of signals so as to simplify the required multiplications. Hagen and Farley (84) have discussed ten different schemes in comparison with full correlation, all of which have been listed in their Table 1.

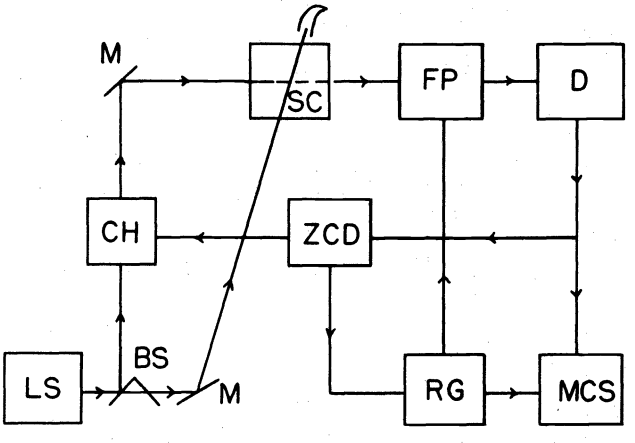


Fig. 8 A typical block diagram for signal-averaging of Rayleigh-Brillouin spectra using a zero-crossing discriminator (41). LS: light source; CH: chopper; SC: sample cell; FP: FP interferometer; D: detection system; ZCD: zero-crossing discriminator; RG: ramp generator; MCS: multichannel scaler; BS: beam splitter; M: mirror.

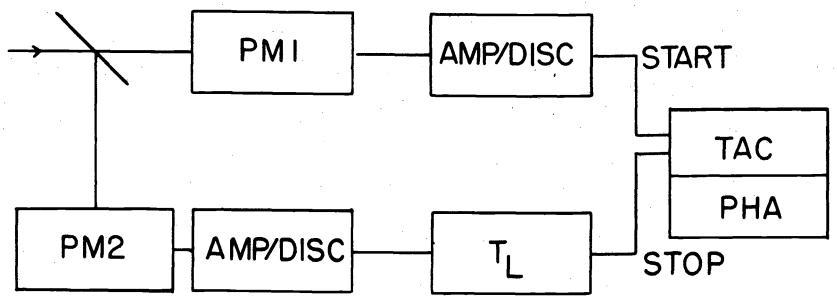


Fig. 9 A schematic diagram for photoelectric correlation measurements with TAC (61). PM: photomultiplier tube; AMP/DISC: amplifier/discriminator; TAC: time-to-amplitude converter; PHA: pulse-height analyzer; TL: delaying discriminator.

Figure 10 shows a generalized correlator. Each correlator channel multiplies a present sample by a delayed sample and stores the product. For analog signals, the data sampler usually includes a signal conditioner and an analog-to-digital converter (ADC). Short-time averages are often performed before ADC by means of resettable charge integrators or RC capacitance integrators. For digital signals, the data sampler is bypassed. In a full correlator, the coarse quantizer is by-passed and we get

$$C(\tau) = \langle n(t,\Delta\tau)n(t+\tau,\Delta\tau)\rangle \tag{8}$$

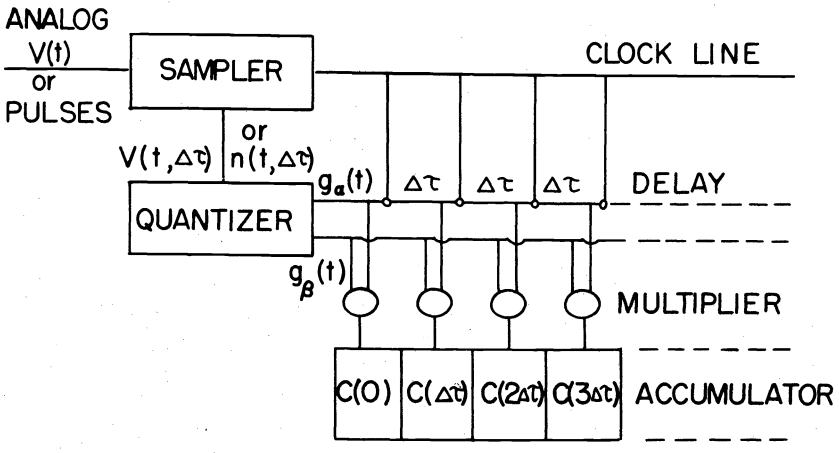


Fig. 10 A block diagram of a generalized correlator. The sampler for analog signals can be an analog-to-digital converter (ADC). The quantizer provides coarse quantization of the signal in order to simplify the required multiplications $C(\tau) = \langle g_\alpha(t)\, g_\beta(t+\tau)\rangle$ is a generalized correlation function. Delay elements can be shift-register flip-flops.

Figure 11 shows some of the transfer functions $g_i(t)$ in quantization schemes for radio astronomy (84). In a one-bit quantization scheme, we have for the time-correlation function

$$C^*_{dc}(\tau) = \langle V_c(t)V_c(t-\tau)\rangle \tag{9}$$

where

$$V_c(t) = 1 \text{ if } V(t)>0$$
$$= -1 \text{ if } V(t)\leq 0$$

The double-clipped auto correlation function $C^*_{dc}(\tau)$, where only polarity information is retained, is related to the actual normalized correlation function via the van Vleck-Middleton (85) condition:

$$\frac{C(\tau)}{C(0)} = \sin\left[\frac{\pi}{2}C^*_{dc}(\tau)\right] \tag{10}$$

Unfortunately, at optical frequencies, only the square of envelope of the signal is detected. Furthermore, the signal is digital and is disturbed by shot noise. Thus, $C(\tau)$ cannot be determined from $C^*_{dc}(\tau)$ by Eq. (10) directly. Table II lists the commonly used correla-

tion functions based on the one-bit coarse quantization scheme. The three-level and two-bit quantization schemes have not been used in macromolecular-dynamics studies.

V 2(b). Advances in hardware correlators. The hardware correlators as listed in Table II have basically the following type of capabilities:

(i) ideal correlator (86) which measures

$$C(\tau) = \langle n(t)n(t+\tau)\rangle = \sum_{n=0}^{\infty}\sum_{n'=0}^{\infty} nn'p(n,n';\tau) \tag{8a}$$

with $p(n,n';\tau)$ being the joint probability distribution,

(ii) add-subtract correlator (50,87,88) which measures

$$C_k^*(\tau) = \langle a_k(t)n(t+\tau)\rangle \tag{11}$$

$$= \sum_{n=0}^{\infty}\sum_{n'=k+1}^{\infty} np(n,n';\tau) - \sum_{n=0}^{\infty}\sum_{n'=0}^{k} np(n,n';\tau)$$

with

$a_k(t) = 1$ if $n(t) > k$; $a(t) = -1$ if $n(t) \leq k$, and

(iii) single-clipped correlator (2,11) which measures

$$C_k(\tau) = \langle n_k(t)n(t+\tau)\rangle \tag{12}$$

$$= \sum_{n=0}^{\infty}\sum_{n'=k+1}^{\infty} np(n,n';\tau)$$

with

$n_k(t) = 1$ if $n(t) > k$; $n_k(t) = 0$ if $n(t) \leq k$

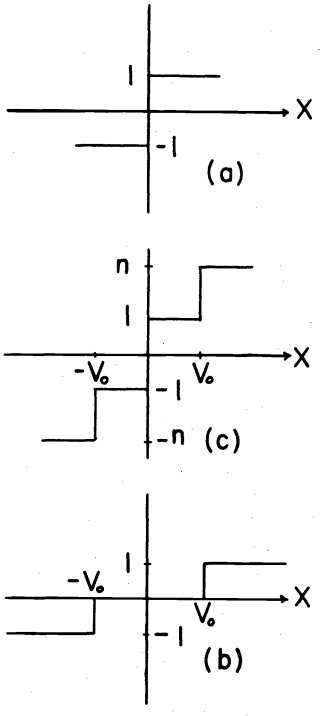


Fig. 11 Coarse quantization schemes

(a) One-bit quantization, polarity detection
(b) three-level quantization
(c) two-bit (four-level) quantization

In a digital single-clipped correlator, the digital pulse signal requires no data sampler (Fig. 10). $g_\alpha(t)$ becomes a clipping gate and $g_\beta(t)$ is the original signal. The delay elements are shift registers and the multipliers are AND gates. The single-clipped correlator has been developed for about six years, is available commercially and can have delay times down to about 50 nsec even though 10 nsec delay times are feasible. No major advances have been made since then. Minor variations include use of monostable circuits as delay elements (89) and more up-to-date integrated circuits (90). Wooding and Pearl (91) have designed a batch processing autocorrelator for analysis of stationary signals with imput frequencies up to 75 MHz. Tai et al. (92) have reported a real time correlator with a peak detector. Their use of temporary memory units is worth noting. Chen et al. (93) has published an improved version of a simple digital clipped correlator for those who have a fast multichannel scaler and some knowledge of digital electronics. An interesting development is in the formulation of add-subtract correlators (50,87,88). Fig. 12 shows a schematic diagram of the preset counter and control circuit for a digital add-subtract correlator (88). It is designed for use with a Tracor Northern NS-906 pulse-height analyzer (23). The circuit is so simple in construction that the estimated cost is less than 100 U. S. dollars for those who have a multichannel scaler and two electronic counters. The add-subtract correlation function is related to the single-clipped correlation function by the expression

$$C_k^*(\tau) = 2\, C_k(\tau) - \langle n \rangle \tag{13}$$

Our add-subtract correlator using a single start-multistop approach measures

$$\hat{C}_k^*(J) = \sum_{\ell=1,\,No+1,\,\ldots}^{N} a_k(\ell)\, n(\ell+J) \tag{14}$$

where $\tau = J\Delta\tau$, $J=1,2,3,\ \ldots\ N_o$ with $N_o$ being the maximum number of data points (or channels), N is the total number of samples, and $N/N_o$ is the total number of scans over the range $\tau$ with $\tau_{max}=N_o\Delta\tau$. Since the single-clipped correlator uses a multistart-multistop approach with

$$\hat{C}_k(J) = \sum_{\ell=1}^{N} n_k(\ell)n(\ell+J) \tag{15}$$

and by virtue of Eq. (13), it takes $N_o/2$ times shorter to accumulate an equivalent amount of data as are provided by the add-subtract correlation function estimate of Eq. (14). On the other hand, $N_o$ can be as high as 1000-2000 channels which will be expensive to duplicate for the parallel single-clipped correlator. Also, it is within reach to construct a multistart-multistop add-subtract correlator whose correlation function estimate is

$$\hat{C}_k^*(J) = \sum_{\ell=1}^{N} a_k(\ell)n(\ell+J) \tag{16}$$

Such a correlator can take full advantage of Eq. (13) and should be twice as efficient when compared with the single-clipped correlator.

V 2(c). Advances in software correlators. General purpose computers cannot formulate the correlation function as fast as hardware correlators or real-time spectrum analyzers. For example, if we take a bandwidth of 1 MHz for the characteristic motion of the macromolecules in solution and want 100 spectral windows. The Nyquist sampling theorem demands a sampling rate of 2 MHz and $N_o$=200. Thus, the rate at which products must be formed and accumulated is $2 \times 10^6 \times 200\ \text{sec}^{-1} = 4 \times 10^8\ \text{sec}^{-1}$ which is about $10^3$ more than the present-day general purpose computers are able to handle on real time. The trick is to retain the quantization scheme and to design a proper front-end so that the computer-controlled system can be quite adequate for many application even though it is not on real time, e.g., one-bit correlation programs have been written for the Arecibo Observatory's CDC3300 computer (84).

In macromolecular dynamical studies, earlier developments (2,94,95) in software correlators used fairly slow analog-to-digital converters (ADC) as the data sampler. Recently, in connection with correlation measurements in a plasma, Ogata and Matsurra (96) have combined a fast buffer memory and a digital computer that can analyze signals with up to 4 MHz bandwidth while Ables et al.(80) have developed a 1024 channel digital correlator that can analyze noise signals with bandwidths up to 10 MHz. The access port from Fig. 6 AS(c) should be adequate. In comparison with Fig. 10, the CPU can act as a hardware correlator and we need a computer with a fast cycle time. Thus, the HP-9830 calculator is much too slow for such operations. For digital pulse signals the data sampler is bypassed. Several other digital autocorrelators using minicomputers have been reported (97-100). In the scheme by Matsumoto et al., (100) the front end consists of a time interval digitizer which digitizes the time intervals between neighboring pulses in a pulse train and transfers the information directly to the core memory through a data channel (DCH). In the

digitizing unit, clock pulses from a 32 MHz crystal oscillator are used to determine pulse intervals ranging from 31.25 nsec to 2.1 sec. Thus, the software correlator is capable of computing $p(n,n',\tau)$ as well as all forms of correlation function with an effective delay time comparable to the fastest hardware correlators, even though it is not truly a real-time system at all delay times. It is, nevertheless, a much more flexible system and offers a greater potential for future development. For example, the method of improving light-beating experiments by dust discrimination (101) requires linking up a hardware correlator with a minicomputer while for the software correlator it becomes merely a subroutine of the software program. Signal conditioning, power spectral analysis, coarse quantization, and batch processing, (102) etc. are many options which many improve the time required for obtaining the correlation function estimate at a preset signal-to-noise ratio. In experiments where real-time operation is not absolutely essential, we can see that a great deal of potential lies with software correlators or firm-ware microprocessors which are less flexible but much cheaper.

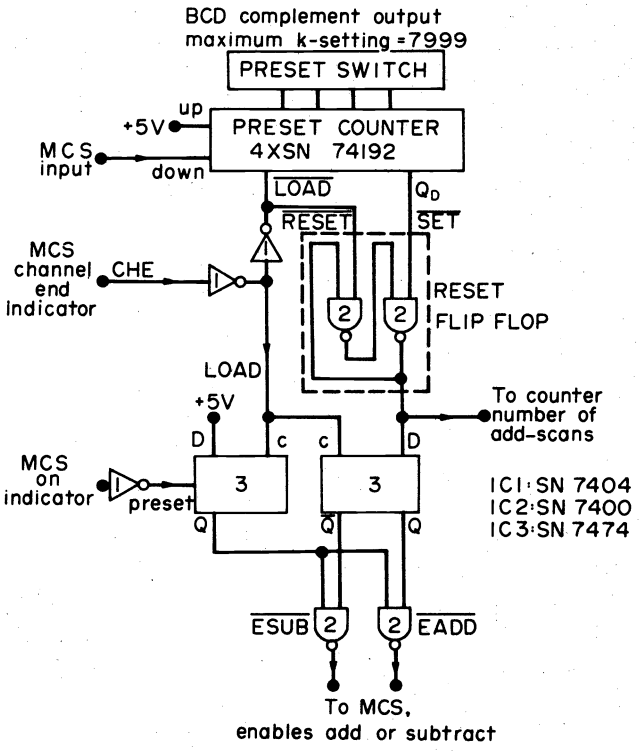


Fig. 12 A block diagram of the preset counter and control circuit for the digital add-subtract correlator (88).

## VI. ADVANCES AND OTHER EFFECTS IN LASER DOPPLER VELOCIMETRY (LDV)

In reviewing advances in the methods of light-scattering spectroscopy for studying dynamical motions of macromolecules in solution, laser Doppler velocimetry represents a fringe area of interest. There have been intensive activities in this field, more so than applications of the technique to polymer science. As LDV is the only measuring technique developed so far which permits determination of flow velocities directly without disturbing the flow itself. Consequently, a brief review of the recent advances in laser Doppler velocimetry is in order. In particular, we want to examine its various optical arrangements which may be applicable in electrophoretic light scattering (2,5,103-105).

Laser Doppler velocimetry has been used to measure the velocity of blood flow in retinal vessels, including the vein and the artery (diameter 120 μm or larger) of rabbits and humans (106-108). Recently a laser Doppler microscope (109-111) has been developed, It can measure flow velocities in capillaries having a diameter less than 10 μm. However, general interests in laser Doppler velocimetry deal with flow at high speeds and turbulence. Wang and Snyder (113) have made an experimental study on the general characteristics of the three commonly used optical arrangements as shown schematically in Fig. 13 (a), (b), and (c). Wang (115) has made a theoretical analysis on (a), (b), and (c) of Fig. 13. Evaluation of techniques in the reference-beam and the cross-beam modes have been derived to handle turbulence measurements, Doppler ambiguity, spatial coherence, and effects of particle concentration and detection aperture (116-118). Tabulated comparisons (115,118)

for different modes of operation reveal the advantages and disadvantages under different experimental conditions. Effects of particle number density on signal-to-noise ratio were also extended to a white light fringe image velocimeter (119). As laser Doppler velocimetry has been more concerned with high-speed flows, such as in a plasma (120), of large particles (~100 μm diam) (121), and in high current arc discharges (122), the standard digital correlator may not necessarily be the best tool. Often signal conditioning and other signal processing approaches or optical arrangements, such as interferometry (122,123), "superheterodyne" spectrum analysis (124), sampling spectrum analysis (125,126), threshold-discriminator-TAC method (127), and count cross-correlation as shown in Fig. 13 (d) are more appropriate. Applications of laser anemometry in transonic and supersonic gaseous flows have been reviewed (128). Aside from standard optical arrangements such as fringe anemometry (cross-beam mode), there is a dual spot technique (129,130) which is particularly suited for observation of back scattered light. It should also be noted that the detector D in Fig. 13 (a), (b), (c) can be a Fabey-Perot interferometer together with the photodetector instead of a light-beating spectrometer.

The more useful aspects of LDV which may be applicable to biological macromolecules in solution are techniques which can tell us additional information on the dynamics of the system. By shifting the incident laser frequency of one of the two beams in Fig. 13 (b) by an acousto-optical method such as the Debye-Sears effect, the LDV can determine the sign of the velocity component (131).

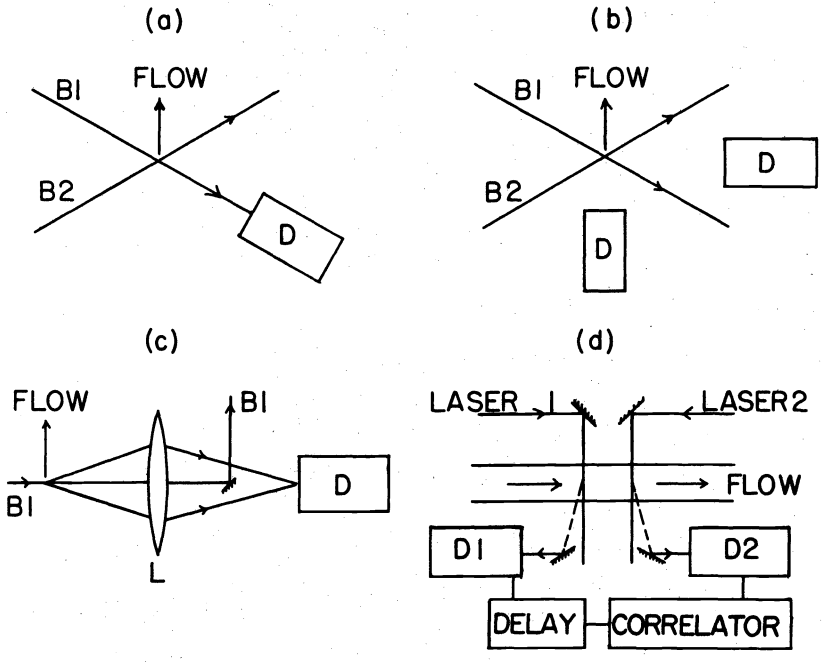


Fig. 13 Schematics of optical arrangements for laser Doppler velocimetry (113,114).
D: photodetector; L: lens.
(a) Local-oscillator heterodyne (reference-beam mode). Beam 1 (B1) is the weak reference beam; beam 2 (B2) is the illuminating beam; $I_{B2} \gg I_{B1}$ with I being the intensity.
(b) Differential heterodyne (cross-beam mode) $I_{B1} \approx I_{B2}$. Photodetector placed along any direction other than the two main beams. The method measures the beating (mixing) of two scattered beams.
(c) Symmetric heterodyne. One incident beam only.
(d) Dual-channel configuration for cross-correlation analysis (114).

Two-component laser Doppler velocimeters have been developed to measure two orthogonal velocity components in periodic flow fields (132-134). Separation of Doppler-shift information into two unambiguous channels has been accomplished by cross polarization and two color optics. Fig. 14 shows a simple beam pattern for a two-dimensional LDV looking towards the laser. In the cross polarization technique, cross-channel interference is not always eliminated completely; but the problem is usually not serious. By adding the frequency shifts, the LDV can measure both velocity components and their polarity.

LDV has been used to measure velocity profiles in a film flow (135). The technique of

tracking (136,137) can be useful for macromolecular fluid flow (138) and aerosol flow studies (139). Finally, fiber optics has been used as a light-scattering probe (140).

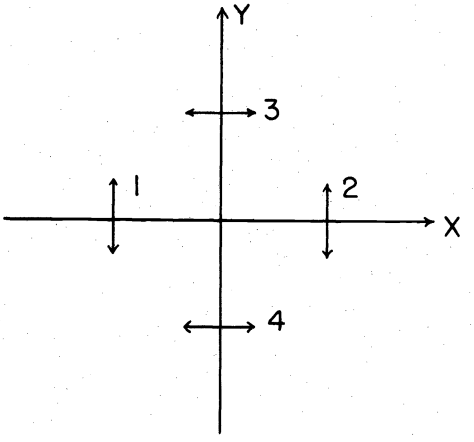


Fig. 14 Beam pattern for a two-dimensional LDV looking towards the laser (132). Arrows indicate the direction of polarization. Beams 1 and 2 measure the X-component and beams 3 and 4 measure the Y-component of flow velocity.

In the field of laser Doppler velocimetry and light-scattering spectroscopy, the engineers again seem to be less aware of the work already published by physicists. For example, a laser anemometer based on an adaptation of the Mach-Zehnder interferometer has been developed (141). The author did not realize that the same optical arrangement was used almost ten years earlier (142). Similarly, in a publication of the use of laser-induced fluorescence in a laser Doppler velocimeter (143), the authors never mentioned the study of reaction kinetics by fluorescence correlation spectroscopy (144). Thus, some improvements in communications between various disciplines that are related to light-scattering spectroscopy may be very helpful to all concerned.

## VII. SUMMARY OF ADVANCES

We have seen that great advances have been made in the methods of light-scattering spectroscopy. The initial development on instrumentation is more or less over. By means of photon-counting and photon correlation, we can have fairly easy access to

(i) measurements of angular distribution of scattered intensity with a resolution about 5-10A,
(ii) computer-controlled Raman spectrometers
(iii) servo mechanisms or zero-cross averaging schemes for the normally stabilized Fabry-Perot interferometers with resolving powers of about $10^8$-$10^9$,
(iv) commercially available hardware correlators which are quite adequate for most dynamical macromolecular studies or instructions for laboratory-built digital autocorrelators, and
(v) flexible computer-controlled software systems which use the same processor (CPU) for (i), (ii) and (iii) as well as photon correlation and spectral analysis. With options for analog input, other forms of probes (145) may be utilized. Furthermore, developments such as a differential technique (146) can easily be adapted. The very diverse nature of the field suggests that we should pay some attention to the advances made by other "related" disciplines.

We now have the basic instrumentation for Rayleigh, Brillouin and Raman scattering. Further improvements are likely in the direction of specific optical arrangements, signal processing and data analysis. In photon correlation, the fitting of superpositions of exponentials by means of least-squares procedures is more difficult and has more pitfalls that it seems to appear. Here, we have very precise experimental data which require further studies in the theory of polymer dynamics. For example, the time-correlation function of DNA cannot be interpreted satisfactorily using simple theories (147). There are much to be done in both theory and method of light-scattering spectroscopy.

Acknowledgments

I gratefully acknowledge support of my research work by the National Science Foundation, the National Institute of General Medical Sciences, the U. S. Army Research Office, the Food and Drug Administration, and the Petroleum Research Fund administered by the American Chemical Society.

TABLE 1. Classification of instruments according to time and frequency domains as well as single and parallel channel methods

| Method | | | |
|---|---|---|---|
| | **Frequency Domain** | | |
| (a) Single channel | Input | Instrument | Example |
| (single start-single stop) | analog | wave analyzer | General Radio[23] 1900 |
| | analog | spectrum analyzer | Tektronix[23] 3L5 |
| (b) Parallel channel | | | |
| (multistart-multistop) | analog | bank of filters | Hewlett-Packard[23,46] 8054 |
| | analog | real-time spectrum analyzer | SAICOR[23] 51B |
| | analog | computer spectral analysis | see text |
| Method | | **Time Domain** | |
| (a) Single channel | | | |
| (i) single start-single stop | digital | delayed coincidence | reference 47 |
| | digital | TAC | reference 48 |
| (ii) single start-multistop | analog/digital | k-gate correlator[(a)] | reference 49,50 |
| (b) Parallel channel | | | |
| (multistart-multistop) | analog/digital | signal correlator | SAICOR[23] 42A |
| | digital | single-clipped correlator | Malvern[23] K7023 |
| | digital | (add-subtract correlator) | see text |
| | analog/digital | computer time-correlation | see text |

(a) The analog version of the digital k-gate correlator is the comparator-trigger autocorrelator.

TABLE 2. Correlation functions based on one-bit quantization

| Input | One-Bit Quantization Scheme | Condition | Correlation Function[a] |
|---|---|---|---|
| V(t), analog | Fig. 11(a) | $V_c(t) = 1$ if $V(t)>0$<br>$= -1$ if $V(t)\leq 0$ | $C^*_{dc}(\tau) = \langle V_c(t)V_c(t+\tau)\rangle$ |
| | | $V_k(t) = 1$ if $V(t)>0$<br>$= 0$ if $V(t)\leq 0$ | $C_k(\tau) = \langle V_k(t)V(t+\tau)\rangle$ |
| n(t), digital | | $a_k(t) = 1$ if $n(t)>k$<br>$= 1$ if $n(t)\leq k$ | $C^*_k(\tau) = \langle a_k(t)n(t+\tau)\rangle$ |
| | | $n_k(t) = 1$ if $n(t)>k$<br>$= 0$ if $n(t)\leq k$ | $C_k(\tau) = \langle n_k(t)n(t+\tau)\rangle$<br>$C_{dc}(\tau) = \langle n_k(t)n_k(t+\tau)\rangle$ |

(a) Subscript dc: double-clipping
subscript k: clipping at k
$C^*_k(\tau)$ : add-subtract correlation function
$C_k(\tau)$ : single-clipped correlation function

REFERENCES


1. P. A. Fleury and J. P. Boon, Advan. Chem. Phys. 24, 1-93 (1973).
2. B. Chu, "Laser Light Scattering," Academic Press, New York (1974).
3. R. Pecora and B. J. Berne, Ann. Revs. Phys. Chem. 25, 233-253 (1974).
4. W. Gelbart, Advan. Chem. Phys. 26, 1-106 (1974).
5. B. R. Ware, Advan. Colloid. Interface Sci. 4, 1-44 (1974).
6. F. D. Carlson, Ann. Revs. Biophys. Bioeng. 4, 243-264 (1975).
7. H. F. P. Knaap and P. Lallemand, Ann. Revs. Phys. Chem. 26, 59-81 (1975).
8. D. R. Bauer, J. I. Brauman and R. Pecora, Ann. Revs. Phys. Chem. 27; (1976).
9. B. Crosignani, P.DiPorto, and M. Bertolotti, "Statistical Properties of Scattered Light," Academic Press, New York (1975).
10. B. J. Berne and R. Pecora, "Dynamic Light Scattering with Applications to Chemistry, Biology and Physics," Wiley-Interscience, New York (1975).
11. H. Z. Cummins and E. R. Pike (eds.) "Photon Correlation and Light Beating Spectroscopy" Plenum Press, New York (1974).
12. C. C. Gravatt, "Light Scattering Methods for the Characterization of Particulate Matter in Real Time," Proceedings of the Conference on Aerosol Measurements, National Bureau of Standards, 7 May 1974.
13. C. Y. She and P. W. Chan, Appl. Opt. 14, 1768 (1975).
14. W. R. McCluney, Rev. Sci. Instrum. 46, 1231 (1975).
15. See Fig. 10.5.3 in p. 285 of reference 2 or Fig. 13 (c).
16. J. H. Lunacek and D. S. Cannell, Phys. Rev. Lett. 27, 841 (1971).
17. S. P. Lee, W. Tscharnuter and B. Chu, Rev. Sci. Instrum. 46, 1278 (1975).
18. E. Gulari and B. Chu, J. Chem. Phys. 62, 798 (1975).
19. C. J. Oliver and E. R. Pike, Appl. Opt. 13, 158 (1974).
20. C. J. Oliver, Appl. Opt. 15, 93 (1976).
21. M. J. E. Golay, J. Opt. Soc. Am. 39, 437 (1947).
22. L. Mandel, Proc. Phys. Soc. 74, 233 (1959).
23. Reference to a company or product name does not imply recommendation of the product nor to the exclusion of others that may be suitable.
24. J. F. Moore, Spex Speaker 14, 1 (1974).
25. R. C. Harney and F. P. Milanovich, Rev. Sci. Instrum. 46, 1047 (1975).
26. R. L. Schwiesow and M. J. Post, Rev. Sci. Instrum. 46, 413 (1975).
27. S. Ushioda, J. B. Valdez, W. H. Ward, and A. R. Evans, Rev. Sci. Instrum. 45, 479 (1974).
28. J. L. Koenig, J. Polymer Sci. Part D, 6, 59 (1972).
29. W. L. Peticolas, Biochimie, 57, 417 (1975).
30. D. J. Evans and S. Ushioda, Solid State Commun. 11, 1043 (1972).
31. S. D. Bloom, R. C. Harney, and F. P. Milanovich, App. Spectrosc. 30, 64 (1976).
32. D. A. Jackson and S. Rajagopal, J. Phys. E. 8, 727 (1975). See also R. H. Callender, Ph.D. Thesis; Harvard University (1969).
33. I. L. Fabelinskii, "Molecular Scattering of Light," Nauka, Moscow (transl. 1968, Plenum, New York) (1968).
34. S. B. Dubin, N. A. Clark, and G. B. Benedek, J. Chem. Phys. 54, 5158 (1971).
35. For example, we have tested and used a Burleigh RC-10 Super-Invar F-P interferometer (23) with very satisfactory results.
36. S. Fray, F. A. Johnson, R. Jones, S. Kay, C. J. Oliver, E. R. Pike, J. Russel, C. Sennett, J. O'Shanghnessy, and C. Smith, in "Light Scattering Spectra of Solids," G. B. Wright, Ed. (Springer-Verlag, Berlin and New York, 1969), pp. 139-150.
37. J. R. Sandercock, Opt. Commun. 2, 73 (1970).
38. R. A. Mclaren and G. I. A. Stegeman, Appl. Opt. 12, 1396 (1973).
39. T. R. Hicks, N. K. Reay, and R. J. Scaddan, J. Phys. E 7, 27 (1974).
40. William G. May, Jr., Burleigh Instruments, Inc. private communication.
41. Q. H. Lao, P. E. Schoen, and B. Chu, Rev. Sci. Instrum. 47, 418 (1976).
42. C. F. Bruce and R. M. Duffy, Rev. Sci. Instrum. 46, 379 (1975).
43. J. H. R. Clarke, M. A. Norman, and F. L. Borsay, J. Phys. E. 8, 144 (1975).
44. N. K. Reay, J. Ring, and R. J. Scaddan, J. Phys. E 7, 673 (1974).
45. D. N. Stacey, V. Stacey, and A. R. Malvern, J. Phys. E. 7, 405 (1974).
46. Y. Yeh, J. Chem. Phys. 52, 6218 (1970).
47. P. N. Pusey and W. I. Goldburg, Appl. Phys. Lett. 13, 321 (1968).
48. H. C. Kelly, J. Phys. A. 5, 104 (1972).
49. S. H. Chen and N. Polonsky-Ostrowsky, Opt. Comm. 1, 64 (1969).
50. Z. Kam, H. B. Shore, and G. Feher, Rev. Sci. Instrum. 46, 269 (1975).
51. C. P. Wang and O. Snyder, Appl. Opt. 13, 98 (1974).
52. D. Meltzer and L. Mandel, IEEE J. Quant. Electronics, QE-6, 661 (1970).
53. P. Ottonello, J. Phys. E. 7, 878 (1974).
54. E. Bodenstedt and J. D. Rogers, in "Perturbed Angular Correlations," (ed. E. Karlsson, E. Mathias, and K. Siegbahn, North Holland Publishing Co., Amsterdam, 1964) Ch. 2.
55. H. Frauenfelder and R. M. Steffen, in "Alpha-, Beta-, and Gamma-Ray Spectroscopy," (ed. K. Siegbahn, North Holland Publishing Co., Amsterdam, 1965) vol. 2.

56. E. Mathias and D. A. Shirley, Nucl. Instrum. Methods 45, 309 (1966).
57. R. W. Zurmuhle, P. F. Hinrichsen, C. M. Fou, C. R. Gould, and G. P. Anastassiou, Nucl. Instrum. Methods 71, 311 (1969).
58. H. H. Rinneberg and D. A. Shirley, Phys. Rev. B. 11, 248 (1975).
59. J. Glatz, Nucl. Instrum. Methods 79, 277 (1970).
60. D. B. Scarl, Phys. Rev. 175, 1661 (1968).
61. F. Davidson and L. Mandel, J. Appl. Phys. 39, 62 (1968).
62. F. Davidson, Phys. Rev. 185, 446 (1969).
63. R. J. Glauber, Phys. Rev. 130, 2529 (1963).
64. L. Mandel and E. Wolf, Rev. Mod. Phys. 37, 231 (1965).
65. R. J. Glauber, in "Fundamental Problems in Statistical Mechanics II," (ed. E. G. D. Cohen, North Holland, Amsterdam, 1968) pp. 140-187.
66. J. G. Blake, "Topics in Photoelectron Counting Statistics," Ph.D. Thesis, Harvard University (1973).
67. S. Chopra and L. Mandel, Rev. Sci. Instrum. 43, 1489 (1972).
68. For example, model 226A of LeCroy Research Systems (23).
69. S. Weinreb, Proc. IRE, 49, 1099 (1961)
70. S. Weinreb, "A digital spectral analysis technique and its application to radio astronomy," M. I. T. Res. Lab. of Electronics, Report 412 (1963), 119 pp.
71. R. M. Goldstein, "A technique for the measurement of power spectra of very weak signals," IRE Trans. Space Electron Telemetry, 8, 2 (1961).
72. R. D. D. Davies, J. E. B. Ponsonby, L. Pointon, and G. DeJager, Nature 222, 933 (1969).
73. B. F. C. Cooper, Aust. J. Phys. 23, 521 (1970).
74. J. M. Moran, Proc. IEEE 61, 1236 (1973).
75. B. G. Clark, Proc. IEEE 61, 1242 (1973).
76. F. K. Bowers, D. A.White, T. C. Landecker, and R. J. Klingler, Proc. IEEE 61, 1339 (1973).
77. A. M. Shalloway, IEEE NEREM Record 6, 98 (1964).
78. C. Bare, B. G. Clark, K. I. Kellermann, M. H. Cohen, and D. L. Jauncey, Science, 157, 189 (1967).
79. W. R. Burns and S. S. Yao, Radio Sci. 4, 431 (1969).
80. J. G. Ables, B. F. C. Cooper, A. J.Hunt, G. G. Moorey and J. W. Brooks, Rev. Sci. Instrum. 46, 284 (1975).
81. D. T. Farley, Radio Sci. 7, 661 (1972).
82. C. L. Rino, M. J. Baron, G. H. Burch, and O. de la Beaujardiere, Radio Sci. 9, 1117 (1974).
83. C. J. Zamlutti and D. T. Farley, Radio Sci. 10, 573 (1975).
84. J. B. Hagen and D. T. Farley, Radio Sci. 8, 775 (1973).
85. J. H. van Vleck and D. Middleton, Proc. IEEE 54, 2 (1966).
86. R. Asch and N. C. Ford, Rev. Sci. Instrum. 44, 506 (1973).
87. P. P. Crooker and J. Hoover, Private Communication (to be published).
88. S. Jen, J. Shook and B. Chu, Rev. Sci. Instrum. (in press).
89. K. Ohbayashi and T. Igarashi, Jap. J. Appl. Phys. 12, 1606 (1973). See also K. Ohbayashi ibid, 13, 1219 (1974) where shift registers were used.
90. A. Mole and E. Geissler, J. Phys. E. 8, 417 (1975).
91. E. R. Wooding and P R. Pearl, J. Phys. E. 7, 514 (1974).
92. I. Tai, K. Hasegawa and A. Sekiguchi, J. Phys. E. 8, 206 (1975).
93. S. H. Chen, W. B. Veldkamp and C. C. Lai, Rev. Sci. Instrum. 46, 1356 (1975).
94. J. M Schurr and K. S. Schmitz, Biopolymers, 12, 1021 (1973)
95. S. A. Shaya, C. CC. Han, and H Yu, Rev. Sci. Instrum. 45, 280 (1974).
96. A. Ogata and K. Matsurra, Rev. Sci. Instrum. 45, 1077 (1975).
97. F. R. Hallett, A. L. Gray, A. Rybakowski, J. L. Hunt and J. R Stevens, Can. J. Phys. 50, 2368 (1972).
98. A. L. Gray, F. R. Hallett and A. Rae, J. Phys. E. 8, 501 (1975).
99. R. W. Wijnaendts van Resandt, Rev. Sci. Instrum. 45, 1507 (1974).
100. G. Matsumoto, H. Shimizu, and J. Shimada, Rev. Sci. Instrum. in press.
101. Y. Alon and A. Hochberg, Rev. Sci. Instrum. 46, 388 (1975).
102. A. Knox and T. A. King, Rev. Sci. Instrum. 46, 464 (1975).
103. E. E. Uzgiris, Rev. Sci. Instrum. 45, 74 (1974).
104. E. E. Uzgiris and J. H. Kaplan, Rev. Sci. Instrum. 45, 120 (1974).
105. J. Josefowicz and F. R. Hallett, Appl. Optics 14, 730 (1975).
106. C. Riva, B. Ross, and G. B. Benedek, Invest. Ophthalmol. 11, 936 (1972).
107. T. Tanaka, I. Ben-Sira, and C. Riva, Science 186, 830 (1974).
108. T. Tanaka and G. B. Benedek, Appl. Opt. 14, 189 (1975).
109. H. Mishina, T. Asakura and S. Nagai, Opt. Commun. 11, 99 (1974).
110. H. Mishina, and T. Asakura, Appl. Phys. 5, 351 (1975).
111. H. Mishina, S. Tokui, T. Ushizaka, T. Asakura, and S. Nagai, Jpn. J. Appl. Phys. Suppl. 14-1, 323 (1975).
112. H. Mishina, T. Koyama, and T. Asakura, Appl. Optics, 14, 2326 (1975).
113. C. P. Wang and D. Snyder, Appl. Optics 13, 98 (1974).
114. T. S. Durrani and C. A. Greated, Appl. Optics 14, 778 (1975).
115. C. P. Wang, J. Phys. E. 5, 763 (1972).

116. C. Y. She, Appl. Opt. 12, 2415 (1973).
117. R. V. Edwards, J. C. Angus, and J. W. Dunning Jr., Opto-Electronics 5, 119 (1973).
118. C. Y. She and L. S. Wall, J. Opt. Soc. Amer. 65, 69 (1975).
119. J. H. C. Chan and E. A. Ballik, Appl. Optics 14, 1839 (1975).
120. G. Gouesbet, C. R. Acad. Sc. Paris, t. 280 Serie B. 597 (1975).
121. A. J. Russo, Appl. Optics 14, 18 (1975).
122. M. R. Barrault, G. R. Jones and T. R. Blackburn, J. Phys. E. 7, 663 (1974).
123. M. Kamegai, Appl. Optics, 13, 1997 (1974).
124. J. Leblond and El. S. El Badawy, Appl. Optics 14, 902 (1975).
125. R. L. Simpson and P. W. Barr, Rev. Sci. Instrum. 46, 835 (1975).
126. G. Gouesbet and M. Trinite, J. Phys. E. 7, 891 (1974); Revue de Physique Appliquee 9, 571 (1974).
127. J. A. Maynard and T K. Gaylord, Rev. Sci. Instrum. 46, 1469 (1975).
128. H. J. Pfeifer, J. Phys. E. 8, 245 (1975).
129. D. H. Thompson, J. Phys. E. 1, 929 (1968).
130. H. Weyer and R. Schodl, "Lecture Series on Experimental Techniques in Turbomachinery," (Milan: Politechnico) (1973).
131. LF. Jernqvist and T. Johansson, J. Phys. E. 7, 246 (1974).
132. J. P. Sullivan and S. Ezekiel, J. Phys. E. 7, 274 (1974).
133. M. K. Denham, P. Briard, and M. A. Patrick, J. Phys. E. 8, 681 (1975).
134. R. J. Adrian, J. Phys. E. 8, 723 (1975).
135. J. Oldengarm, A. H. van Krieken and H. W. van der Klooster, J. Phys. E. 8, 203 (1975).
136. T. H. Wilmshurst and J. E. Rizzo, J. Phys. E. 7, 924 (1974).
137. W. R. Tompkins, R. Monti, and M. Intaglietta, Rev. Sci. Instrum. 45, 647 (1974).
138. R. V. Mustacich and B. R. Ware, Rev. Sci. Instrum. 47, 108 (1976).
139. M. K. Mazumder and K. J. Kirsch, Appl. Optics 14, 894 (1975).
140. B. T. Yang and R. N. Meroney, Rev. Sci. Instrum. 45, 210 (1974).
141. J. E. Rizzo, J. Phys. E. 8, 47 (1975).
142. J. B. Lastovka and G. B. Benedek, Phys. Rev. Lett., 17, 1039 (1966).
143. W. H. Stevenson, R. dos Santos, and S. C. Mettler, Appl. Phys. Lett., 27, 395 (1975).
144. D. Magde, E. Elson, and W. W. Webb, Phys. Rev. Lett., 29, 705 (1972); Biopolymers 13, 29 (1974).
145. G. Feher and M. Weissman, Proc. Nat. Acad. Sci. USA 70, 870 (1973).
146. D. S. Cannell and S. B. Dubin, Rev. Sci. Instrum. 46, 706 (1975).
147. F. C. Chen, A. Yeh, and B. Chu, J. Chem Phys., in press.